An Electrically Active Microneedle Array for Electroporation of Skin for Gene Delivery

Seong-O Choi[1], Jung-Hwan Park[1, 2], Yoonsu Choi[1], Yeuchun Kim[2], Harvinder S. Gill[3], Yong-Kyu Yoon[1], Mark R. Prausnitz[2, 3], and Mark G. Allen[1, 2]
[1]School of Electrical and Computer Engineering, Georgia Institute of Technology,
[2]School of Chemical and Biomolecular Engineering, Georgia Institute of Technology
[3]Wallace H. Coulter Department of Biomedical Engineering, Georgia Institute of Technology

ABSTRACT

We have designed and fabricated a microneedle array with electrical functionality with the final goal of electroporating skin's epidermal cells to increase their transfection by DNA vaccines. The microneedle array was made of polymethylmethacrylate (PMMA) by micromolding technology from a master PDMS mold, followed by metal deposition, patterning using laser ablation, and electrodeposition. This microneedle array possessed sufficient mechanical strength to penetrate human skin *in vivo* and was also able to electroporate red blood cells as an *in vitro* model to demonstrate cell membrane permeabilization.

Keywords: Microneedle, Electroporation, Gene delivery, Laser ablation, Micromolding

INTRODUCTION

One approach to gene therapy is to deliver DNA vaccines to cells in the skin's outer layer of epidermis. Due to the presence of Langerhans dendritic cells, DNA vaccines administered to skin can elicit a strong immune response [1]. This method of gene therapy is limited in part by the need to improve DNA delivery into cells for increased gene expression in the skin.

Electroporation is known to increase gene transfection based on extensive *in vitro* work and more recent success *in vivo* [2]. To improve on previous work, the challenge in this study was to develop a method to locally cause electroporation of epidermal cells using a device appropriate for eventual clinical use.

For *in vivo* electroporation, typically either plates or needle electrodes have been used, and electroporation is performed under high voltages ranging from several hundred volts to even several thousand volts depending on the gap between electrodes.

Our collaborator, Cyto Pulse Sciences, is addressing this challenge by adapting microneedles developed for transdermal drug delivery to serve as microelectrodes for minimally invasive, highly-localized electroporation of the epidermis (Fig. 1) [3]. As envisioned by Cyto Pulse Sciences, microneedles could serve two functions for gene therapy of skin. By coating with DNA, microneedles could first serve as a vehicle to deliver DNA to epidermis. While microneedles remain inserted in skin, they could subsequently serve as microelectrodes to locally electroporate epidermal cells. Previous studies have shown that microneedles can be painlessly inserted into skin. Moreover, the close spacing of the microneedle electrodes means that the large electric fields needed for electroporation can be achieved at relatively low voltages.

In this paper, we present the fabrication of an electrically active microneedle array using micromolding and laser ablation techniques, and the lysis of red blood cells by electroporation to verify its electrical functionality.

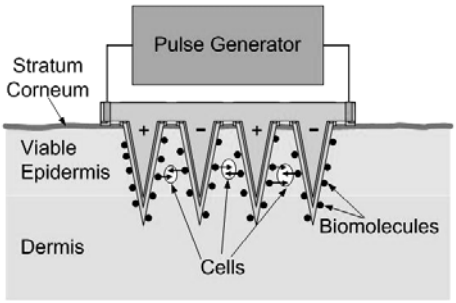

Fig. 1. Conceptual use of microneedle electrode array to electroporate cells in epidermis and thereby increase expression of DNA vaccines [3].

DEVICE FABRICATION

Devices are fabricated by mold replication from a micromachined master. To fabricate the master structure, SU-8 is spun on a glass substrate bearing an array mask pattern, baked, and then exposed from the backside to form a tapered microneedle array [4,5] (Fig. 2). Needles are sharpened by RIE etching. A polydimethylsiloxane (PDMS) mold is then copied from the master (Fig. 2(a)). A PMMA microneedle array (Fig. 3) is formed by solvent-casting, and then released from the mold (Fig. 2(b)). To realize electrical functionality, a Ti/Cu seed layer is deposited on the PMMA microneedle array and patterned by excimer laser to electrically isolate adjacent rows (Fig. 2(c)). A 25μm thick Ni layer for enhanced structural rigidity is electroplated on the patterned seed layer (Fig. 2(d)). A backside electrical connection to the array is formed by backside etching of a hole and forming electrical connection through the hole (Fig. 2(e)).

Since the final microneedle structure is created by molding, it is possible to contemplate a variety of materials as the microneedle substrate. Candidate

materials lie at the intersection of moldability into high aspect ratio molds and biocompatibility. In this work, PMMA was chosen as it satisfied both these criteria. An additional advantage of the molding approach is its inherent mass-producibility, important for ultimate disposable applications; it is possible to reproduce the structure easily and quickly compared to a conventional photolithography process using SU-8.

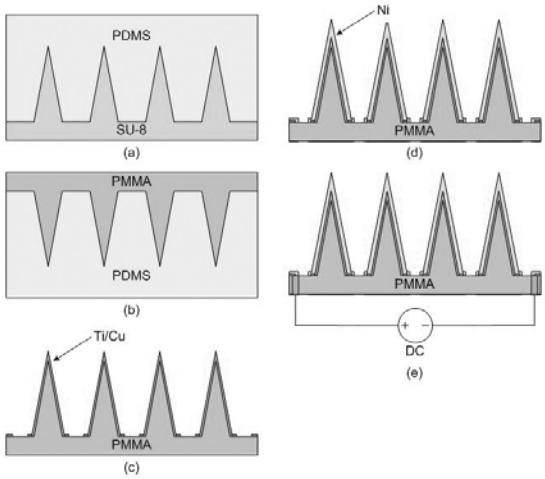

Fig. 2. Schematic diagram of fabrication process.

In the micromolding of high aspect ratio structures, it is often difficult to utilize conventional thermoplastic melt-molding to form the structure from highly viscous polymer due to of the potential for bubble entrapment in the deep and narrow mold. For our microneedle array, PMMA powder (M_W=75,000, Scientific Polymer Products Inc., USA) was dissolved in ethyl l(-)-lactate (Acros Organics, USA), which is a relatively lower toxicity solvent compared to many other PMMA solvents. Due in part to the reduction of viscosity achieved by polymer solution, void-free molding and subsequent microneedle replication was successfully fabricated as shown in Fig. 3. An additional advantage of the solvent-casting method is that it requires lower processing temperatures than thermoplastic molding. However, although the appropriate geometries were achieved using this process, the mechanical strength of the PMMA-only structure was insufficient to reproducibly survive a skin-insertion test. This issue was successfully addressed by metal coating as described below.

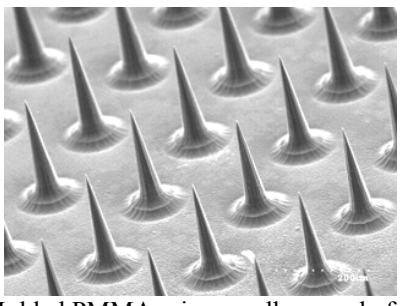

Fig. 3. Molded PMMA microneedle array before addition of electrical functionality.

Fig. 4 shows a device containing a 16x16 array of electrically active microneedles, with adjacent microneedle rows electrically isolated. The height of the microneedles is 400µm, bottom diameter is 100µm, and pitch between microneedles is 250µm. Deposition of a seed layer of metal (Ti/Cu, 300Å/3000Å) on the array was performed using DC sputtering. Careful control of sputtering parameters is required to avoid problems of substrate deformation during sputtering. The seed layer was patterned by excimer laser ablation to isolate adjacent microneedle rows with a 100µm gap. After isolation, a 25µm thick Ni layer was electrodeposited at room temperature with stirring to enhance structural rigidity. For electrical connection between the microneedle array and external electroporation electronics, a backside contact is required so as to not interfere with insertion of the array into skin. To achieve this contact, a via was formed from the backside of the PMMA substrate using a CO_2 laser. Copper wire was then passed through the via and connected to the underside of the metallization using silver paste followed by an epoxy mechanical connection.

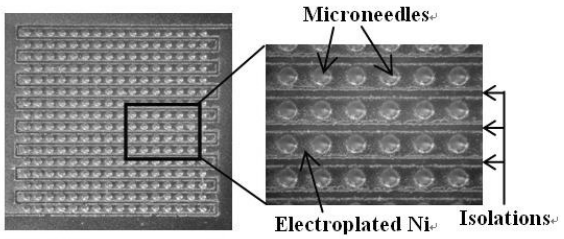

Fig. 4. Photomicrograph of a 16x16 active microneedle array, showing an interdigitated pattern for electrical isolation between rows.

EXPERIMENTAL METHODS AND RESULTS

We first needed to determine if the microneedle electrodes fabricated for this study had appropriate mechanical properties to insert into skin. Microneedles will mostly be subjected to axial forces during their insertion into skin. Yield stress of the microneedle array to an axial load was determined by using a force-displacement testing station (Tricor Systems, USA). The microneedle array was attached to the specimen holder of the force-displacement test station and then pressed against a rigid metal surface at a rate of 1.1 mm/s. Stress versus strain curves were then extracted from the measured force vs. displacement data. The failure force of the microneedle array was also determined from the force versus displacement data by correlation to a sudden drop in measured force, which represents the failure point. The microneedle array was examined under microscope before and after the test to determine the mode of failure.

For the solvent-cast PMMA microneedle array, the average failure force per microneedle was 0.018N. With addition of 25µm thick Ni, the mechanical strength of the microneedle array is significantly improved and the

failure force was measured to be 0.7N. Previous tests have shown that microneedles of this geometry insert into skin with a force of 0.01N, which means that Ni-coated needles should be sufficiently robust for transdermal applications.

To examine the skin penetration ability of the microneedle array, several insertion tests were performed on human subjects using either non-coated (polymer-only) PMMA microneedles or nickel-coated PMMA microneedles of various nickel thicknesses. While a polymer-only array could not penetrate through human skin, a PMMA microneedle array with a 10μm thick electrodeposited Ni layer was sufficiently strong. However, it was observed that these needles were bent after several successive insertions. Thicker 25μm-thick coated arrays were therefore tested. Upon removal from skin, the skin was stained with blue dye and then observed by microscopy. Fig. 5 shows the stained skin in the pattern of the microneedle electrode array, indicating that the microneedle electrodes pierced into the skin. Subsequent microscopic examination of the arrays showed that microneedle electrode tips were not damaged, even after multiple insertions (Fig. 6).

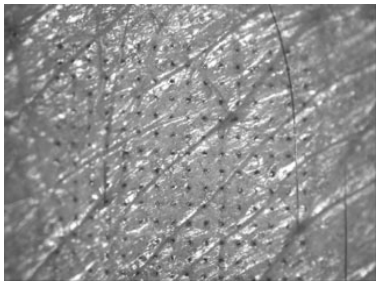

Fig. 5. Photomicrograph of human skin *in vivo* after piercing with microneedle electrodes and staining with blue dye.

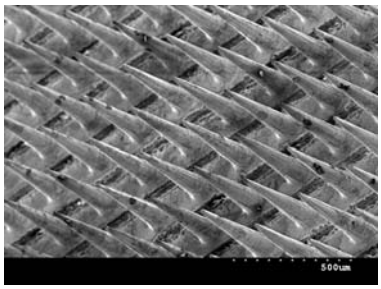

Fig. 6. SEM picture of microneedle array after multiple insertion tests. Tissue debris is shown on the surface of intact microneedles.

To test the electroporation ability of the microneedle array, an *in vitro* red blood cell (RBC) lysis assay was performed. This assay provides an easy way to quantify the electroporation effect. Upon electroporation, the RBCs rupture and release their hemoglobin into solution which can be easily quantified by absorption spectroscopy.

Approximately 20 ml of bovine blood in alsevers anticoagulant (Rockland Inc., USA) was measured into a 50 ml polypropylene centrifuge tube. Phosphate buffered saline (PBS) was added to the tube which was then centrifuged at 236G for 10 minutes. The supernatant was then discarded and approximately 20 ml more PBS was added for another wash. A total of three PBS washes were done, after which the supernatant was discarded and a resultant RBC pellet was formed. The microneedle array under test was affixed to a surface with the microneedles facing up. The array was connected to electrical circuitry to provide a controlled electroporation pulse with an exponential decay waveform. For each electroporation experiment, 25μl of concentrated RBC pellet was pipetted onto the microneedle array. Three different peak voltage levels of 53, 108 and 173 volts each were applied each using (i) 1 pulse with an exponential decay time constant $\tau = 0.5$ ms, (ii) 3 pulses with $\tau = 0.5$ ms and (iii) 1 pulse with $\tau = 1$ ms.

After pulse application, the 25μl RBC suspension was pipetted off into a centrifuge tube. An additional 1ml PBS was added to the tube and centrifuged at 735G for 5 min. After centrifugation, 700μl of the supernatant was collected for quantifying the amount of hemoglobin using absorption spectroscopy. A negative control was prepared by repeating this procedure but without the application of the electrical pulse. A positive control was also prepared by adding 1 ml deionized water to 25μl of RBC pellet. This causes osmotic rupture of all RBCs. All experimental conditions were repeated three times to generate triplicate data points. A total of two identical microneedle arrays were used to perform the electroporation experiments. The arrays were washed with PBS between each electroporation experiment.

Hemoglobin in the samples was quantified using absorption spectroscopy at 575 nm absorption wavelength. To perform these measurements, 200μl of sample was pipetted into a 96 well plate (Costar flat bottom, Fisher). The amount of hemoglobin in the samples was then calculated as a percentage of positive control which is reported as RBC lysis (%). The results have been normalized by multiplying by a factor of 3.9 to account for difference in volume of RBC applied onto the array (25 μl) and the effective volume available for electroporation (approximately 6.4 μl).

Results from RBC electroporation via microneedles are shown in Fig. 7. The figure summarizes all the electroporation conditions used. Percent RBC lysis is represented along the y-axis and the results are grouped on the x-axis according to the voltage applied. There is a statistically significant increase in electroporation of RBCs as the applied voltage increases ($p<0.0001$). Electroporation of as high as 84% was achieved at 173 V and 1 pulse with 1 ms pulse duration. A separate ANOVA analysis was performed to identify the effect of pulse length and pulse duration on electroporation. Results from this ANOVA show that RBC lysis increases with both pulse length and pulse duration ($p<0.0001$).

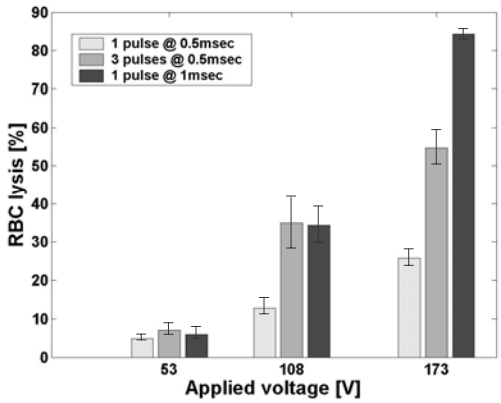

Fig. 7. Hemoglobin released from red blood cells after electroporation using the microneedle electrode array

The ultimate application of these microneedle electrode arrays is to cause reversible electroporation of living cells in the skin and thereby transfect those cells with DNA. Figure 7 demonstrated electroporation of RBCs to cause cell lysis. Because this irreversible electroporation of RBCs is phenomenologically related to reversible electroporation of skin cells, we have used this assay as a first test of microneedle electrode device performance. Future studies will address the ability of these devices to reversibly electroporate living cells and its effect on DNA transfection.

ELECTRIC FIELD SIMULATION

A 3-D finite element (FE) model was created using FEMLAB 3.1 to examine the electric field distribution around the microneedle array. To mimic the real device, the model consists of 16 microneedles with the same geometrical parameters as the microneedle array, and 4 microneedles located at the center of the model were analyzed. Fig. 8 shows the top view the of electric field distribution at a height of 100μm, approximately the height where the viable epidermis is located. The simulation results demonstrated that with 100V applied between two adjacent rows, a maximum field strength of approximately 10kV/cm near the microneedle electrodes was generated. This field strength is thought to be too high for electroporation for delivering biomolecules, while it is suitable for cell lysis. At the middle of two adjacent rows, the field strength was about 4kV/cm. These field strengths scale with the applied voltage and can therefore be optimized for specific applications (not shown). However, implicit in this design are "dead regions" where electroporation cannot occur between two microneedles with the same electric potential. It is therefore desirable to optimize the geometry of the microneedle array through further FE analysis. By doing so, we can reduce the effective areas of both the "highly active" and "dead" regions, which will in turn lead to both high rates of biomolecule delivery via electroporation and high survival rates of electroporated cells.

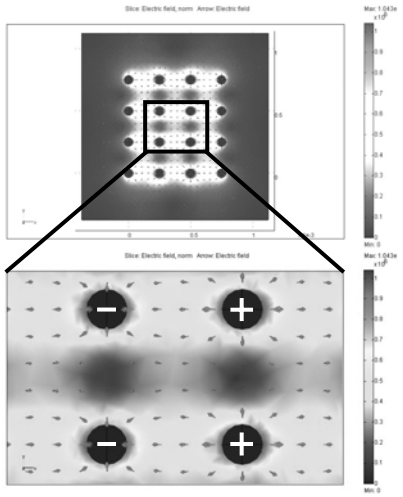

Fig. 8. FEM simulation of electric field distribution

CONCLUSIONS

This study demonstrated the fabrication and molding-based replication of microneedle arrays made of polymer, coated with a metal layer, and etched to act as alternating electrodes suitable for electroporation of epidermal cells. Experiments in human subjects established that microneedle electrode arrays are strong enough to insert into skin. Additional experiments with red blood cells showed that these microneedle electrodes are electrically active and capable of electroporating cells.

ACKNOWLEDGEMENTS

This work was supported in part by NIH. The authors would like to thank Dr. Jin-Woo Park for helpful discussions regarding microneedle array fabrication.

REFERENCES

[1] K. K. Peachman, M. Rao, C. R. Alving, "Immunization with DNA through the skin," *Methods*, **31**, 232-42 (2003).

[2] M. J. Jaroszeski, R. Heller, and R. Gilbert, Electrochemotherapy, Electrogenetherapy, and Transdermal Drug Delivery, Humana Press, Totowa, NJ, 2000.

[3] A. D. King, R. E. Walters, "Delivery of macromolecules into cells," *U.S.Patent* 6,603,998, 2003.

[4] J. Park, Y. Yoon, M. R. Prausnitz, and M. G. Allen, "High-aspect-ratio tapered structures using an integrated lens technique," *Proc. 17th IEEE Int. Conf. MEMS*, pp. 383-6, Maastricht, Netherlands, Jan. 25-29, 2004.

[5] K. Kim, D. S. Park, H. M. Lu, W. Che, K. Kim, J. Lee, and C. H. Ahn, "A tapered hollow metallic microneedle array using backside exposure of SU-8," *J. Micromech. Microeng.*, **14**, 597-603 (2004).